# Quantification of drug metabolising enzymes and transporter proteins in the paediatric duodenum via LC-MS/MS proteomics using a QconCAT technique

Goelen, Jan; Farrell, Gillian; McGeehan, Jonathan; Titman, Christopher M; J W Rattray, Nicholas; Johnson, Trevor N; Horniblow, Richard D; Batchelor, Hannah K

*DOI:*
10.1016/j.ejpb.2023.08.011



*Document Version*
Publisher's PDF, also known as Version of record

*Citation for published version (Harvard):*
Goelen, J, Farrell, G, McGeehan, J, Titman, CM, J W Rattray, N, Johnson, TN, Horniblow, RD & Batchelor, HK 2023, 'Quantification of drug metabolising enzymes and transporter proteins in the paediatric duodenum via LC-MS/MS proteomics using a QconCAT technique', *European Journal of Pharmaceutics and Biopharmaceutics*, vol. 191, pp. 68-77. https://doi.org/10.1016/j.ejpb.2023.08.011

European Journal of Pharmaceutics and Biopharmaceutics 191 (2023) 68–77

Contents lists available at ScienceDirect

European Journal of Pharmaceutics and Biopharmaceutics

journal homepage: www.elsevier.com/locate/ejpb

Research paper

# Quantification of drug metabolising enzymes and transporter proteins in the paediatric duodenum via LC-MS/MS proteomics using a QconCAT technique

Jan Goelen [a,b], Gillian Farrell [b], Jonathan McGeehan [c], Christopher M. Titman [c], Nicholas J. W. Rattray [b], Trevor N. Johnson [d], Richard D. Horniblow [e], Hannah K. Batchelor [b,*]

[a] School of Pharmacy, University of Birmingham, Birmingham B15 2TT, UK
[b] Strathclyde Institute of Pharmacy and Biomedical Sciences, University of Strathclyde, Glasgow G4 0RE, UK
[c] Shimadzu UK Ltd, Milton Keynes, MK12 5RE, UK
[d] Simcyp Division, Certara UK Limited, Sheffield, UK
[e] School of Biomedical Science, University of Birmingham, Birmingham B15 2TT, UK

A B S T R A C T

Characterising the small intestine absorptive membrane is essential to enable prediction of the systemic exposure of oral formulations. In particular, the ontogeny of key intestinal Drug Metabolising Enzymes and Transporter (DMET) proteins involved in drug disposition needs to be elucidated to allow for accurate prediction of the PK profile of drugs in the paediatric cohort.

Using pinch biopsies from the paediatric duodenum (n = 36; aged 11 months to 15 years), the abundance of 21 DMET proteins and two enterocyte markers were quantified via LC-MS/MS. An established LCMS nanoflow method was translated to enable analysis on a microflow LC system, and a new stable-isotope-labelled QconCAT standard developed to enable quantification of these proteins. Villin-1 was used to standardise abundancy values. The observed abundancies and ontogeny profiles, agreed with adult LC-MS/MS-based data, and historic paediatric data obtained via western blotting. A linear trend with age was observed for duodenal CYP3A4 and CES2 only. As this work quantified peptides on a pinch biopsy coupled with a microflow method, future studies using a wider population range are very feasible. Furthermore, this DMET ontogeny data can be used to inform paediatric PBPK modelling and to enhance the understanding of oral drug absorption and gut bioavailability in paediatric populations.

## 1. Introduction

The small intestinal physiology changes with age [1,2], and as such, pharmacokinetic (PK) profiles observed in adult populations following administration of an oral drug may not always directly extrapolate to what would be observed in paediatric populations. For many oral drugs, this approximation of the pharmacokinetic profiles in children is undertaken, since clinical trials in the paediatric population are challenging due to ethical constraints [3], logistical challenges [4], larger inter-individual variability [5,6] or safety issues [6]. A route to overcome poor predications and make better estimations is the use of physiologically-based pharmacokinetic (PBPK) modelling [7–9] and is of great value. PBPK software packages typically integrate drug characteristics and formulation properties with population-based anatomical-physiological data to mechanistically predict the pharmacokinetic (PK) profile of a drug [10]. For this, accurate and representative biophysiological input data are essential. Paediatric PBPK models require additional information on organ development and ontogeny of pathways involved in drug disposition [11]. Oral drug disposition prediction tools have been developed as part of these [12], however this has been hampered due to minimal availability of robust anatomical-physiological information and oral paediatric pharmacokinetic data [13].

Characterising key intestinal parameters will progress the development of paediatric PBPK tools by incorporation of accurate population data from the subjects of interest. One of these key parameters is the abundance of intestinal drug metabolising enzymes and transporter proteins (collectively, DMET proteins) in the gut lumen [14,15]. In general, 21 intestinal DMET proteins (Table 1) are of interest due to their clinical relevance and impact on the PK profile of a large number of drugs (CYP enzymes are involved in the metabolism of nearly 70% of drugs administered to children [16]). This list of 21 is generated based on recommendations from scientific consortia (such as the Paediatric Transporter Working Group [17] or the International Transporter

* Corresponding author.
*E-mail address:* hannah.batchelor@strath.ac.uk (H.K. Batchelor).

https://doi.org/10.1016/j.ejpb.2023.08.011
Received 17 March 2023; Received in revised form 13 August 2023; Accepted 18 August 2023
Available online 23 August 2023

**Table 1**
The 21 target DMET proteins of specific interest in this project and two markers.

| Transporter proteins | CYP enzymes | UGT enzymes | Other enzyme | Markers |
|---|---|---|---|---|
| ABCB1; P-gp; MDR1 | CYP2C9 | UGT1A1 | CES2 | $Na^+/K^+$-ATPase |
| ABCC2; MRP2; cMOAT | CYP2C19 | UGT1A3 | | VIL1 |
| ABCC3; MRP3 | CYP2D6 | UGT1A4 | | |
| ABCC4; MRP4 | CYP2J2 | UGT1A8 | | |
| ABCG2; BCRP | CYP3A4 | UGT1A9 | | |
| SLC15A1; PEPT1 | CYP3A5 | UGT2B7 | | |
| SLC22A1; OCT1 | | UGT2B17 | | |

Consortium [14,18,19]). Additionally, most of these proteins have previously been quantified in adult and paediatric intestinal tissue [20–23].

Membrane-bound drug transporter proteins facilitate migration or actively transport compounds across the membrane, and thus are important regulators for drug disposition following oral absorption [16,17,24]. They are located within the plasma membrane of the enterocyte, as are the enterocyte-markers villin-1 (VIL-1) [25] and Na–/$K^+$-ATPase [26]. Drug metabolising enzymes, like cytochrome P450 (CYP)-enzymes, uridine 5′-diphospho (UDP)-glucuronosyltransferases (UGTs) and carboxylesterase 2 (CES2) [27], metabolise endogenous and xenobiotic compounds and are located in the enterocyte in the cytosol or embedded in the membrane of the endoplasmic reticulum.

Currently, there are inadequate data on paediatric intestinal DMET proteins to infer ontogeny of their expression. From the limited data that does exist, it is derived from mRNA analysis or immunochemical assays, which are sub-optimal for quantifying protein abundance [28]. Western blotting can have a low sensitivity, especially with very small samples, however CYP3A4 [29] has been estimated using this technique and did show a reasonable correlation between protein abundance and activity *in vitro*, based on the rate of conversion of testosterone to 6β-hydroxytestosterone in small bowel S9 fractions. Similarly, mRNA concentration is not necessarily linked to protein content or activity [30], so has disconnection between mRNA and protein levels for transporter ABCC2 been demonstrated previously [31], highlighting the need for a more sensitive and more accurate quantification method.

Using a more sensitive approach, such as liquid chromatography-tandem mass spectrometry (LC-MS/MS), would enable these low-abundant DMET proteins to be simultaneously and accurately quantified from small tissue samples. Detection of a peptide sequence that uniquely belongs to a single protein (proteotypic) allows for surrogate detection of that protein. Additionally, quantification of the proteotypic peptides is possible using heavy-isotope-labelled copies of the proteotypic peptides [32–35]. To date, only one report of paediatric intestinal DMET proteomic data is available [20], yet such data is in high demand for the development of oral paediatric drug tools. DMET proteins have been quantified in adult liver and GIT using a QconCAT [21,32,36,37] (an artificial protein concatenating all proteotypic peptides of interest). Typically, large tissue samples were used, obtained as surgical waste or derived from donors [21,32,33,38,39] (the smallest biopsy size reported in previous LC-MS/MS studies was 100 mg). Only one paper reports using pinch biopsies to quantify GIT DMET proteins, where two rectal mucosal pinch biopsies per participant were used (25 mg average weight) to quantify UGTs only [40]. Using a QconCAT as heavy standards reduces cost and time when analysing multiple (approximately 10–50) protein targets in multiple (approximately 20–100) samples [41,42]. QconCATs have been used previously to quantify DMET-proteins in adult small intestine (TransCAT [32] and MetCAT [21,43]). However, this approach has not yet been applied for DMET quantification in the paediatric GIT. This is the first work to report the feasibility to determine the abundance of important DMET-proteins in paediatric intestinal pinch biopsies using a QconCAT as heavy standard and a high-end standard LC MS/MS system using a microflow system.

## 2. Methods

### 2.1. Tissue collection

Paediatric duodenal pinch biopsies were collected from children younger than 15 years old during endoscopic procedures, which were part of their clinical care. Informed consent by a parent, guardian or those with legal responsibility for the child in their care was obtained in every case. The biopsy forceps had a diameter of 1.8 mm when opened, resulting in biopsies with a theoretical surface area of 2.54 $mm^2$. Immediately after collection, the biopsies were frozen at −80 °C for further processing. Ethical approval was granted by the South Birmingham NRES Committee (*IRAS 251909*). Tissue processing and LC-MS/MS analysis were performed blinded to subject diagnosis or demographics. The participants were stratified into age groups according to the ICH classifications [44,45], using following age ranges: <2 years: neonate/infants, 2–5 years: pre-school children, 6–11 years: school-age children, 12–16 years: adolescents.

### 2.2. Protein extraction from biopsies

All protein extraction steps were performed at 4 °C. A list of chemicals used and manufacturers is given in **Supporting Information (SI) Table 1**. The frozen biopsies were crushed to a fine powder in a pre-cooled pestle and mortar with liquid nitrogen ($LN_2$). The pulverised tissue was resuspended with Radio-Immunoprecipitation Assay (RIPA) lysis/extraction buffer, containing IGEPAL CA-630 1% (v/v), sodium deoxycholate 0.5% (w/v), sodium dodecyl sulfate 0.1% (w/v) and a protease inhibitor cocktail (1 tablet per 50 mL solution, according to the manufacturers instruction). The resuspension was snap-frozen in $LN_2$ and stored at −70 °C. The lysate resuspensions were thawed at 4 °C with agitation on a rotating shaker (30 min, 25 rpm). Samples were then sonicated for 5 sec before centrifugation (9 000 *g*, 5 min, 4 °C) and the supernatants collected. The protein concentration in the supernatant fraction was determined using Pierce's BCA protein assay according to the manufacturer's instructions.

### 2.3. PaedCAT design and expression

A stable-isotope-labelled "heavy" standard in the form of a QconCAT (named PaedCAT (Polyquant, Bad Abbach, Germany)) was used for quantification of the peptides of interest and to correct for potential variation in sample preparation procedures. The selection of proteotypic peptides to include on PaedCAT (**SI Table 2**) was based on literature and shotgun-experiments performed on a protein digest of a mucosal protein fraction obtained from adult colonic tissue (processed in the manner described above, ethical approval: Birmingham Human Biomaterials Resource Centre, REC: 20/NW/0001 and RG_HBRC21-379).The selected peptide sequences fulfilled the selection criteria defined by Kamiie *et al.* [46].

For every target protein (Table 1), 2 to 3 proteotypic peptides were encoded into PaedCAT. One peptide sequence (TYSTSYTLEDLDR) was shared between UGT1A8 and UGT1A9. By also measuring a peptide uniquely coding for UGT1A9 (AFAHAQWK), UGT1A8 levels could be determined using the difference between the abundance of both peptides as done previously by Couto [21]. A list of the target peptides in the correct order as present on the QconCAT can be found in **SI Figure 1**.

### 2.4. Protein digestion via FASP

Protein concentrations were diluted using RIPA to obtain a 1 µg

protein/μL solution. From this, 20 μg of total mucosal protein was mixed with 370 μL urea (UA) buffer (8 M urea in 0.1 M Tris/HCl, pH 8.5) and 10 μL of the QconCAT PaedCat solution (200 fmol/μL) was added. The mixture was vortexed for 30 sec, then, 40 μL of a 100 mM 1,4-dithiotreitol (DTT) in UA buffer (pH 8.5) was added to the sample, followed by incubation at 56 °C for 40 min. The FASP-filter unit was primed according to the manufacturer's instruction. After the denaturing and reduction step, the cooled mixture was transferred to the filter unit and the sample was centrifuged at 14,000 *g* for 20 min at room temperature (RT) and the filtrate was discarded. Next, 400 μL of the UA buffer was added, together with 20 μL of freshly prepared 300 mM iodoacetamide (IAA) in UA buffer (pH 8.5). This alkylation step was performed in the dark for 30 mins. After this, the sample was spun at 14,000 *g* for 20 min at RT and the filtrate discarded. The sample was washed by adding 400 μL UA buffer (pH 8.5) and spinning at 14,000 *g* for 20 min at RT, discarding the filtrate. Next, three washing steps were included to reduce the urea concentration in the sample, by adding 400 μL of 50 mM ammonium bicarbonate (ABC) in ultrapure water and spinning at 14,000 *g* for 20 min at RT, discarding the filtrate (repeated three times). Tryptic digestion of the proteins was assisted by Lys-C digestion: enzyme solution 10 μL (0.2 mg/mL enzyme) (Trypsin/Lys-C Mix, Mass Spec Grade, Promega) and 30 μL of a 25 mM ABC-solution were added to the FASP filter. The samples were incubated at 37 °C under agitation (105 rpm) overnight.

Elution of the peptides was performed by adding 50 μL of 100 mM ABC, 5% acetonitrile and spinning at 14,000 *g* for 20 min at RT twice, collecting the filtrate for every sample. The eluates were acidified by adding 2 μL of 10% trifluoroacetic acid (TFA). Next, the digests were desalted by using $C_{18}$ pipette tips according to the manufacturer's instructions. The samples were then dried using a Speed-Vac (45 °C) (Concentrator 5301, Eppendorf) and stored at −80 °C until batch quantification by LC-MS/MS.

### 2.5. LC-MS/MS based quantification of proteotypic peptides

Concentrations of the endogenous (light) peptides were analysed by LC-MS/MS in relation to the heavy spiked-in peptides. Samples were reconstituted as followed: 20 μg dried mucosal peptides were resuspended in 35 μL of a buffer composed of 98% (v/v) LC-MS-grade water (with 0.1% (v/v) formic acid (FA)) and 2% acetonitrile (with 0.1% (v/v) FA). The samples were placed in an autosampler (Shimadzu Nexera, SIL-40C X3 at 4 °C), 25 μL of the reconstituted sample was injected onto the column. Peptide separation, detection and quantificationparameters used in the final LC-MS/MS method are listed in Table 2.

Prior to sample analysis, final peptide, precursor and fragment selection and instrument setting optimisation (collision energy, ion focussing voltage, loop time) were performed, via an iterative approach of method development, result analysis and subsequent method refinement. SI Table 3 lists the final selection of peptides monitored for LC-MS/MS based quantification (together with transitions and expected retention time).

**Table 2**
Detailed parameters of the LC-MS/MS method.

| Item | Details |
|---|---|
| Column | C18, ACQUITY Premier Peptide, 100 × 2.1 mm, 1.8 μm, Waters, UK |
| Oven | Shimadzu Nexera CTO-40C at 30 °C |
| Flow rate | 0.5 mL/min |
| Mobile phase A | LC-MS grade ultrapure water with 0.1% (v/v) FA |
| Mobile phase B | LC-MS grade acetonitrile with 0.1% (v/v) FA |
| Mobile phase gradient | Shimadzu Nexera LC-40D XS Binary System and Solvent Delivery Module |
| | **Time (min)** 0 2 42 47 53 55 |
| | **Mob. Phase B (%)** 3 3 70 95 3 3, end |
| Triple quadrupole | Shimadzu LCMS 8060NX, MRM setting |
| Ionisation mode | Electrospray Ionisation (ESI) |
| MRMs per peptide | Usually 4 (range 3–6) |
| Acquisition window | 96 s around the expected retention time |
| Dwell time | 5 msec |
| Pause time | 3 msec |
| Loop time (max) | 1.442 s |

The endogenous signal was assessed based on peak profile and number of transitions co-eluting with the heavy standard. Since the target proteins were potentially low in abundance, a minimal limit of three co-eluting light transitions with adequate peak shape (i.e. peak clearly differentiating from the background noise) was set. If these conditions were not met, the endogenous signal was excluded from further analysis. Additionally, samples were excluded if either the light or heavy signal for villin-1 was not observed. The linearity of the MS signal over the range of the expected protein amount was assessed using calibrators. As background matrix, a HeLa cell digest was used (yet only the heavy MS channel belonging to PaedCAT was observed, the light MS channel for native peptides ignored). The calibrators ranged from 0.1 to 2000 fmol/μL, where the expected range of DMET-protein abundance was 1–200 fmol/μL.

Skyline (version 21.2.0.568) was used for method development and optimisation, together with the LC-MS/MS instrument-specific software LabSolutions (version 5.109). Skyline and Microsoft excel (version 1808) were used for data analysis and visualisation. The built-in method optimisation feature in Skyline has been employed to optimise the collision energy (Collision Energy Optimisation).

### 2.6. Protein abundance calculation

The light-to-heavy ratio for every peptide was normalised to the light-to-heavy ratio of the enterocyte marker villin-1. Correction to villin-1 is commonly done to normalise for the heterogeneity of intestinal tissue samples [29,47–49], and villin-1 is not reported to be influenced by ontogeny [20,29]. The villin-1 light-to-heavy ratio is derived from the signal of peptide DPETPIIVV**K**. (Note: the blue letter in bold signifies the stable isotope arginine or lysine).

$$villinnormalisedratio_{ij} = \frac{RatiopeptideL/H_{ij}}{RatiovillinL/H_j}$$

***Equation 1.*** *Normalisation of the light-to-heavy signal ratio (L/H) of peptide i in sample j is done by division of the original peptide ratio to the light-to-heavy signal ratio of the marker villin-1, given by peptide DPETPIIVV**K**, in sample j. For clarity, the marker villin-1 is written as "villin".*

- The normalised ratios were then multiplied to the initial PaedCAT amount spiked in the sample (2000 fmol in 20 μg protein, or 100 fmol per μg protein).

$$Protein_iabundanceinsample_j = villinnormalisedratio_{ij} * 100 \frac{fmol}{\mu g} protein$$

***Equation 2.*** *Protein abundance for a certain target protein in the sample (given in fmol/μg protein) is obtained by multiplying the villin-1 normalised light-to-heavy peptide ratio with the amount of PaedCAT spiked in, 100 fmol per μg protein. For clarity, the marker villin-1 is written as "villin".*

This allowed for single-point quantification of protein abundances based on the signal ratio of the endogenous (light) to PaedCAT-standard (heavy) peptides.

### 2.7. Statistical analysis of protein abundancy data

Statistical analysis was performed using the software packages IBM SPSS (version 28.0.1.1) and GraphPad Prism (version 9.4.1). The following statistical tests were employed:

- To investigate correlations of protein abundance with age and correlations between protein abundances, the nonparametric Spearman correlation was used.
- To investigate differences between more than two groups of samples, a Kruskal-Wallis test was performed.

Statistical tests were deemed significant at $p < 0.05$.

## 3. Results

### 3.1. Tissue collection

Duodenal biopsies were collected from 36 paediatric participants. The participants ranged from 11 months to 15 years old, with a final diagnosis as healthy for 21 children, 12 children with underlying disease and 3 without a final diagnosis communicated. SI Table 4 gives an overview of the demographics, reason for endoscopy and final diagnosis of the paediatric participants included in this study.

On average, the paediatric pinch biopsies had a mass of 17.85 mg (standard deviation (SD) 6.41 mg, median 16.7 mg), with a range of 8.4 mg to 32.1 mg, which is in line with literature reports for pinch biopsy sizes [50].

### 3.2. PaedCAT design and expression

A QconCAT (named PaedCAT) containing proteotypic peptides for 21 target proteins and markers was developed by Polyquant GmbH.

### 3.3. Protein digestion via FASP and peptide selection

Proteins were digested into peptides using trypsin and Lys-C in a FASP protocol. In one sample (UK053) there was insufficient protein remaining for LC-MS quantification following the BCA assay.

For five proteins (ABCB1, ABCG2, UGT1A1, UGT2B17 and UGT2B7), two peptides were suitable for quantification (i.e. a qualitative heavy and light peptide signal recorded). The light-to-heavy ratios of the two peptides of UGT2B7 are in close correlation, which is also the case for two peptides of UGT1A1 ($p < 0.05$ for both) (see SI Figure 2). However, this was not the case for the peptides for ABCB1 and ABCG2 ($p > 0.05$ for both, SI Figure 3). Thus, the protein data reported (Table 3) is based on the signals for every individual peptide. Representative co-elution profiles are given in SI Figure 4, repeatability of retention times in SI Figure 5; repeatability of fragment contribution to peak area in SI Figure 6 and representative calibration curves given in SI Figure 7. Linear regression of signal versus amount PaedCAT injected onto the MS gave a close correlation of > 0.97 for all peptide targets, except for peptides ITILVTHQLQYLK (ABCC4) (R2 = 0.05), NITFFSTNCVEGTAR (ATP1A3) (R2 = 0.67), VQQCGIHSK (SLC15A1) (R2 = 0.32) and EVSVVDILSHASVWLFR (UGT1A3) (R2 = 0.00). The first two peptides were excluded before data collection, and no endogenous signal was observed for the latter two peptides, hence no data needed to be excluded post-analysis.

**Table 3**
DMET-protein abundance in paediatric duodenum. Values are expressed in pmol/mg protein. N shows the number of samples in which the protein was quantified (out of a total of 34, 11 months-15 years old), SD standard deviation.

| Protein | N | Minimum | Maximum | Mean | SD |
|---|---|---|---|---|---|
| CES2 | 34 | 33.36 | 132.34 | 77.70 | 23.91 |
| CYP2C19 | 33 | 0.58 | 5.41 | 2.18 | 1.12 |
| CYP2C9 | 34 | 1.33 | 6.60 | 2.36 | 0.97 |
| CYP2D6 | 31 | 0.51 | 7.79 | 2.18 | 1.54 |
| CYP3A4 | 32 | 4.80 | 31.89 | 17.57 | 7.03 |
| CYP3A5 | 31 | 1.36 | 10.43 | 4.32 | 2.23 |
| UGT1A1[a] | 30 | 6.60 | 30.79 | 15.52 | 5.46 |
| UGT1A1[b] | 32 | 1.85 | 98.83 | 11.84 | 16.57 |
| UGT2B17[c] | 28 | 4.19 | 61.32 | 28.14 | 12.39 |
| UGT2B17[d] | 34 | 1.43 | 106.30 | 36.93 | 25.10 |
| UGT2B7[e] | 28 | 1.99 | 11.56 | 4.96 | 2.35 |
| UGT2B7[f] | 33 | 1.14 | 6.28 | 2.59 | 1.03 |
| ABCB1[g] | 32 | 0.46 | 6.28 | 1.50 | 1.08 |
| ABCB1[h] | 32 | 0.57 | 4.22 | 1.57 | 0.82 |
| ABCC2 | 31 | 0.56 | 5.73 | 1.75 | 1.13 |
| ABCG2[i] | 19 | 0.49 | 1.89 | 1.11 | 0.45 |
| ABCG2[j] | 24 | 1.32 | 10.12 | 4.11 | 2.05 |
| SLC22A1 | 23 | 1.59 | 17.50 | 5.20 | 3.55 |

Using [a]: DGAFYTLK, [b]: TYPVPFQR, [c]: FSVGYTVEK, [d]: SVINDPIYK, [e]: IEIYPTSLTK, [f]: TILDELIQR, [g]: AGAVAEEVLAAIR, [h]: FYDPLAGK, [i]: LFDSLTLLASGR, [j]: VIQELGLDK as probe to infer protein abundance for these five proteins with two proteotypic peptides.

### 3.4. Protein abundancy data

The ratio light-to-heavy for villin-1 (given by peptide DPETPIIVVK) spanned a 12-fold difference in range (mean: 0.57 ± 0.29, range 0.13–1.5). Villin-1 was detected in all but one sample. Table 3 summarises the protein abundancy of the quantified proteins in 34 paediatric intestinal biopsies, the data for individual samples is given in SI Table 5. Out of 21 target proteins, 13 could be quantified (with addition of two markers). Not all proteins were expressed in all samples and this is shown as the N number in Table 3.

#### 3.4.1. Abundance of DMET proteins and ontogeny

*3.4.1.1. CYP enzymes and CES2.* It was possible to quantify 5 out of 6 Cytochrome P450 isoform targets in the paediatric duodenum. A qualitative endogenous signal for CYP2J2 was not observed in any sample for either target peptide. The mean (and SD) of the different CYP and CES2 protein abundances for the entire paediatric cohort and per age group are given in Fig. 1.

The measured proteins were in following rank order for the entire paediatric cohort: CYP3A4 > CYP3A5 > CYP2C9, CYP2D6, CYP2C19 in comparable levels (Fig. 2**A**).

The protein abundance between the different age groups (2–5 year old, 6–11 and older than 12) were compared via Kruskal-Wallis tests. Infants were excluded as there was only one participant (11 months old) in this cohort. The Kruskal-Wallis test was not significant for any protein. Significant correlations were observed for age and the protein abundance of CES2 and CYP3A4 (Spearman's correlation 0.440, $p = 0.009$ for CES2 and Spearman's correlation 0.381, $p = 0.032$ for CYP3A4) (Fig. 2**B**). Non-significant correlations between the abundance of other proteins and age on continuous scale were found.

*3.4.1.2. Transporters.* Out of the 7 transporter proteins included in the assay, 4 could be quantified. No endogenous signal was observed for basolateral efflux transporters ABCC3 and ABCC4, or for the peptide transporter PEPT1 (SLC15A1). SLC22A1 was the most expressed transporter, ABCC2 and ABCB1 were expressed in similar levels (Fig. 3**A**). However, the rank order of ABC-transporters could not be determined, as ABCG2 is either the most or the least abundant ABC-transporter depending on which proteotypic peptide for protein quantification is used. Similarly, two peptides were suitable for quantification for ABCB1 (SI Figure 3), so the results for both proteins are reported using two proteotypic peptides.

*3.4.1.3. UGT enzymes.* Three from the seven targeted UGT enzymes were quantified in paediatric duodenum. For UGT1A3, UGT1A4, UGT1A8 and UGT1A9 no endogenous signal was observed. UGT2B17 was the most expressed enzyme, followed by UGT1A1 and UGT2B7. For all three quantified proteins, two proteotypic peptides were used (SI Figure 2). Quantifying the protein abundance with either proteotypic peptide does not influence the overall rank order of the UGT enzymes as observed in Fig. 3**B**.

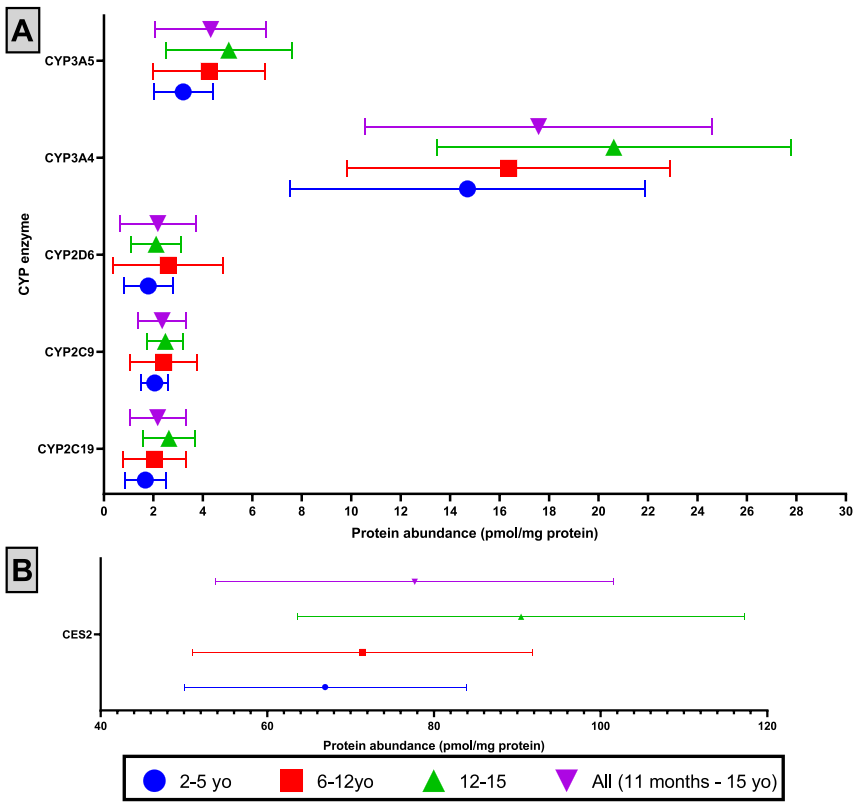


**Fig. 1.** **(A)** CYP and **(B)** CES2 enzyme protein abundance in paediatric duodenum for the entire cohort and different age groups. Symbols depict the mean, error bars denote the SD.

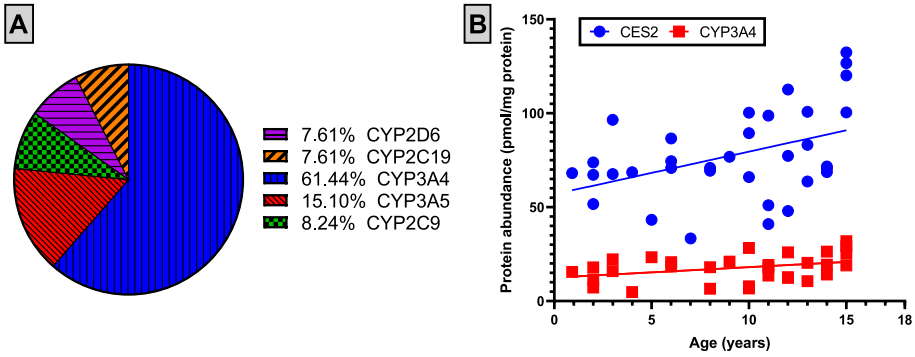


**Fig. 2.** **(A)** Mean relative abundance of the quantified CYP enzymes in paediatric duodenum of 34 participants across all age groups. **(B)** Correlation between age and the protein abundance of CES2 and CYP3A4. (Spearman's correlation 0.44 and 0.381 for CES2 and CYP3A4 respectively, $p < 0.05$ in both cases).

### *3.4.2. Interprotein correlations*

Pairwise protein abundance correlations were tested using the nonparametric Spearman test. Strong significant Spearman correlations ($r > 0.5$, $p < 0.05$) are listed in Table 4. The abundance of all transporter proteins are correlated with each other.

## 4. Discussion

### *4.1. CYP enzymes and CES2 abundance*

CYP3A4 was the most abundant CYP enzyme identified within the paediatric duodenum, followed by CYP3A5, and similar levels were detected for CYP2C9, CYP2D6 and CYP2C19. An identical rank order is reported from adult intestinal tissue [21], with CYP3A4 the most expressed CYP enzyme [48,51–53] followed by CYP2C9 and comparable levels of CYP2D6, CYP2C19 and CYP2J2 [21,54]. CYP levels for the eldest age group (12–15 year old) in the paediatric duodenum are comparable to reported values in adult duodenum, jejunum and ileum (Fig. 4**A** for CYP3A4, **SI Table 6** for all target CYP enzymes). Visual inspection of the graphical data presented in Kiss *et al.* [20] confirms CYP3A4 as the most abundant CYP-enzyme in paediatric jejunum and ileum.

For younger age groups, the abundancy of CYP3A4 in paediatric duodenum is similar to the values reported by Johnson *et al* [29], obtained via western blots on 104 paediatric samples (Fig. 4**B**). A significant increase of CYP3A4 with age was observed on continuous scale (Fig. 2**B**), but no statistical difference was found between different age groups. An increase of CYP3A4 with age was also reported by proteomic analysis on paediatric jejunum and ileum [20]. No statistically significant effect of age on expression of other CYP enzymes has been found in the present study, nor for UGT-enzymes and transporter proteins. A significant trend with age for CES2 duodenal expression was observed in

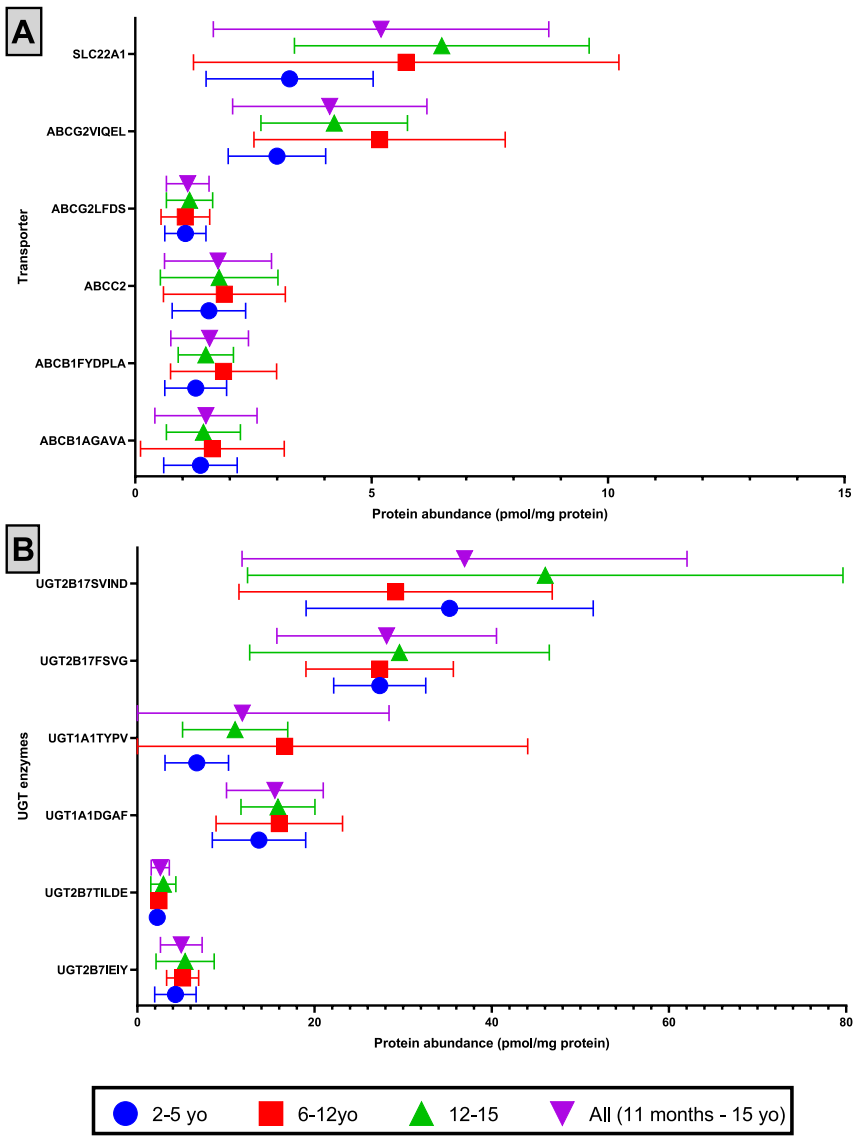


**Fig. 3.** **(A)** Transporter and **(B)** UGT enzyme protein abundance in paediatric duodenum for the entire cohort and different age groups. Symbols depict the mean, error bars denote the SD.

this study, which corroborates previous results via mRNA and protein level in the paediatric duodenum [55]. This also correlates with ontogeny of hepatic CES2, and an increase in dietary esters and amides [56,57]. Thus, as the QconCAT approach has been validated for adult intestinal DMET proteomics, the transferability on paediatric tissue has been demonstrated, even with a higher LC flowrate which enables access to a wider range of apparatus.

The higher bioavailability (i.e. lower intestinal metabolism) of oral midazolam in young children can be linked to this ontogeny of CYP3A4. Midazolam is a benzodiazepine frequently used in neonatal and paediatric medicine for sedation [58,59]. Midazolam is metabolised by intestinal and hepatic CYP3A4, and its PK-PD profile is extensively studied in children [60–66]. Adult bioavailability is reported to be around 30% [67], whereas high bioavailability (92.1%, range 67–95%) was observed in preterm neonates [68].

It needs to be noted, although a similar trend with age is observed for CYP3A4, the reported abundance values for CYP3A4 by Kiss *et al.* (0–2 year olds: 75.6 ± 64.05 pmol/mg protein) are very dissimilar from the values reported in Johnson *et al.* or this study (Fig. 4**B**). Additionally, the adult abundancy values reported in their paper do not resonate with other studies for adult intestine. For example, Kiss reported adult jejunum CYP3A4 abundance as 536 ± 588.1 pmol/mg protein (mean ± S.D.), compared to 33.33 ± 570 pmol/mg protein in Couto's publication. These discrepancies could be due to differences in sample preparation and analysis protocol [69–71].

An example on how sample preparation procedures influence the abundancy data is demonstrated in Groer *et al* [39]. Here, pooled human intestinal microsomes were examined for their CYP- and UGT-content. One set of intestinal microsomes was prepared in-house, a second set were commercially acquired. Although both sets of microsomes were derived from macroscopically healthy jejunal tissue and were prepared for LC-MS in the same laboratory and analysed on the same instrument, a large difference in e.g. CYP3A4-content was observed. Gröer hypothesised the differences in abundance to be due to dissimilar microsomal isolation procedures. It is recognised that interlaboratory differences between intestinal DMET abundance are associated with the different methodological approaches in the proteomic workflow to quantify intestinal DMET-abundance [21]. LC-MS apparatus-set-up can also influence obtained abundancy data as by reported differences in abundancy values by Couto [21] and Al-Majdoub [43]. Here, the same samples were analysed, with one protocol using a targeted MS approach using QconCATs as heavy standard. The other protocol used a semi-targeted

**Table 4**
Spearman r for significant interprotein correlations observed in paediatric duodenum ($p < 0.05$ for all). Blank fields indicate non-significant ($p > 0.05$) interprotein correlations.

| | ABCB1[b] | ABCC2 | ABCG2[c] | ABCG2[d] | ATP1A1 | CYP2C19 | CYP2C9 | CYP2D6 | CYP3A5 | SLC22A1 | UGT1A1[e] | UGT2B17[f] | UGT2B17[g] | UGT2B7[h] |
|---|---|---|---|---|---|---|---|---|---|---|---|---|---|---|
| ABCB1[a] | 0.68 | 0.64 | 0.62 | 0.57 | 0.62 | | 0.66 | 0.39 | 0.56 | 0.51 | | | | |
| ABCB1[b] | | 0.78 | 0.79 | 0.69 | 0.68 | 0.53 | 0.66 | 0.74 | 0.73 | 0.68 | 0.52 | | | 0.76 |
| ABCC2 | | | 0.60 | 0.69 | 0.71 | | 0.65 | 0.75 | 0.65 | 0.66 | 0.61 | | | 0.76 |
| ABCG2[c] | | | | | | | 0.68 | | 0.65 | | | | | 0.58 |
| ABCG2[d] | | | | | | | 0.69 | 0.68 | 0.58 | 0.55 | | | | |
| ATP1A1 | | | | | | 0.62 | 0.74 | | 0.67 | 0.66 | 0.69 | | | 0.64 |
| CES2 | | | | | | 0.53 | 0.59 | | | | | | | |
| CYP2C19 | | | | | | | 0.63 | | 0.67 | | 0.56 | 0.60 | 0.54 | |
| CYP2C9 | | | | | | | | | 0.60 | 0.62 | 0.58 | | | 0.70 |
| CYP2D6 | | | | | | | | | 0.52 | 0.63 | 0.58 | | | 0.60 |
| CYP3A4 | | | | | | | | | | | | 0.54 | | |
| CYP3A5 | | | | | | | | | | 0.51 | 0.55 | | | 0.52 |
| SLC22A1 | | | | | | | | | | | 0.64 | | | 0.73 |
| UGT1A1[e] | | | | | | | | | | | | | | 0.71 |
| UGT2B17[f] | | | | | | | | | | | | | 0.85 | |

Protein concentration assessed by proteotypic peptide: [a]: AGAVAEEVLAAIR, [b]: FYDPLAGK, [c]: LFDSLTLLASGR, [d]: VIQELGLDK, [e]: DGAFYTLK, [f]: FSVGYTVEK, [g]: SVINDPIYK, [h]: IEIYPTSLTK.

approach where identification was based on accurate mass and retention times (AMRT), quantification relied on the ion peak intensity of heavy and light version across samples, with the relative abundance interpolated from the intensity ratios [43,72]. The difference in reported abundance for CYP3A4 are ten-fold, with 33.33 (±5.7) pmol/mg for the target approach, in contrast to 2.47 (±2.68) pmol/mg for the AMRT method. However, this does not fully explain the observed differences with Kiss *et al.* as a target approach was also used. The differences observed by Kiss compared to this study may be explained by a number of factors including the type of heavy peptides used; the fact that Kiss used intestinal tissue samples but did not isolate enterocytes; the use of tissue samples from diseased paediatric patients or the method used to normalise to villin.

Some proteins, such as CYP2J2, were not quantified in any paediatric duodenal biopsy. Despite a well-observed signal for the heavy standard, no endogenous signal was detected. CYP2J2 has been quantified before via LC-MS/MS in adult intestine [51], where intestinal tissue samples were taken from recently diseased adults due to head trauma, with or without GIT comorbidities. The expression of CYP2J2 significant increased along the small intestine, with lowest expression in the duodenum. Expression of CYP2J2 is closely correlated with CYP2C9 and CYP2D6 in adult intestine [21,73], the latter two were quantified in paediatric duodenum. Thus, potentially a mixed effect of ontogeny and disease effect on the expression of CYP2J2 in the lowest expression region may explain the lack of endogenous signal, although no ontogeny for CYP2J2 has been reported.

### 4.2. Transporter protein abundance

In this study, similar levels of ABCC2 (MRP2) and ABCB1 (P-gp) were observed. ABCG2 (BCRP) was either the most or least abundant ABC-transporter, depending on which of the proteotypic peptides was selected for quantification. A similar trend (ABCG2 > ABCB1 > ABCC2) was also observed using proteomics in adult jejunum and ileum [32,48] and via immunoquantification in the adult duodenum [74]. However, conflicting trends in adult jejunum/ileum have also been reported, such as ABCC2 > ABCB1 > ABCG2 [21,22,33], or ABCB1 > ABCC2 > ABCG2 [33] (**SI Table 7**)). No ontogeny of ABCB1 has been observed in this study, in agreement of existing literature on mRNA expression or immunoquantification of proteins [75–79] or paediatric proteomics [20]. Kiss *et al.* [20] reported a significant trend with age for ABCG2 abundance, but this is not supported by the findings in this study or existing mRNA data [76]. No effect of age has been observed in this study for the duodenal abundance of ABCC2,. However, Kiss *et al.* showed ontogeny, their study included samples from 29 participants aged 0–2 years, in our study only one such sample was collected. Obtaining more paediatric duodenal samples for DMET-quantification, with additional efforts for the youngest cohort, could further elucidate ontogeny profiles that were not observed in this study, as the major intestinal changes happen within the first two years of life [16].

Potentially, intestinal ABC-transporters are challenging to quantify. In Harwood *et al.* [32], using a selective procedure to isolate the enterocytes from the underlaying tissue layers, ABCB1 and ABCC2 were below the limit of quantification. In Kiss *et al.* [20], the mean ileal ABCG2 abundance is lowest in the 12–18 year old group, with higher expression levels for the 0–2 age group and highest for adults. No other evidence for such an ontogeny function has been reported. Similarly, it was challenging to find a final abundance value for ABCB1 and ABCG2, as the endogenous signals of the two probes for either protein were not correlating. This could be due to dissimilar chemical stability characteristics of the peptides. In this study, the chemical stability of the proteotypic peptides in human matrices was not investigated, although similar work reports adequate stability of peptide samples upon reconstitution [32,33,39]. Additionally, uncharacterised protein isoform or detected posttranslational modifications can also explain this discrepancy [39]. However, it is still useful to report the protein abundance

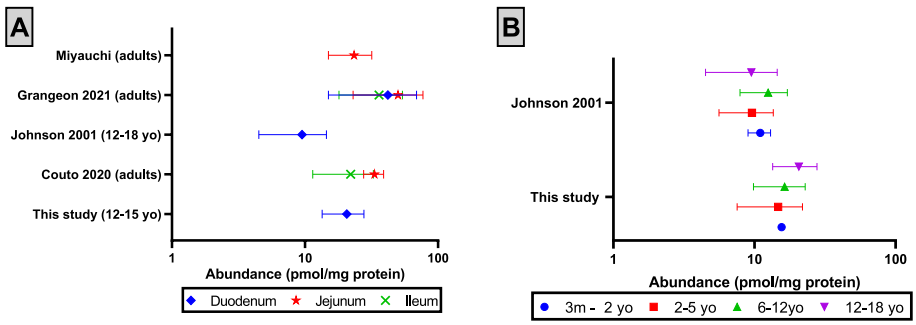


**Fig. 4.** **(A)** Intestinal CYP3A4 abundance values for the eldest age group in this study (12–15 years old (yo)) and key publications on adult intestinal proteomics. *: the results by Johnson et al. [29] are based on western blotting. Symbols indicate mean, error bars denote the SD. **(B)** Reported CYP3A4 abundance in this study and Johnson et al. across different age groups. Symbols indicate the mean, error bars denote the SD.

assessed by both probes, as this can give tools used for drug prediction a wider range to model with, so extreme values would be covered. As such, there is no clear consensus on the abundance and rank of ABC-transporters.

In adult duodenum, the reported abundance for SLC22A1 (OCT1) is $0.7 \pm 0.35$ pmol/mg [22], in a previously study on paediatric duodenum around 5–10 pmol/mg. Values similar to the latter are found in this study for SLC22A1 ($5.20 \pm 3.55$ pmol/mg protein), using the identical proteotypic probe. However, no endogenous signal for SLC15A1 (PEPT1) was observed for any sample despite MS-optimisation based on the internal standard. As endogenous signal for SLC15A1 has been observed in paediatric and adult intestinal tissue [20,22,33] with different probes, the chosen proteotypic peptide here was potentially not optimal. SLC15A1 shares substrate specificity with basolateral efflux transporters ABCC3 and ABCC4 [80], neither were detected in this study. The expression of these ABC-transporters has been reported to increase along the GIT with highest levels observed in the adult colon [22,31,33].

### 4.3. UGT enzyme abundance

The observed rank order for the UGT-enzymes that were quantified in paediatric duodenum was UGT2B17 > UGT1A1 > UGT2B7. This correlates to the observed rank orders in adult intestine (**SI Table 8**) [21,33,48]. Previously, a significant difference has been reported for the UGT1A1 abundance in the ileum and jejunum of 0–2 year olds compared to adults; however no difference with age was observed here. This could be due to limited number of infant biopsies available as previously described.

#### 4.3.1. Method development, strengths and limitations

It is a strength of this study to be the first to successfully quantify three different DMET-protein families using pinch biopsies, as most studies use larger surgical waste tissue or diseased donors [20,31,51], isolated intestinal mucosa sections [21] or only examined one sub-family of DMET proteins (e.g. cell membrane isolation [31–33] or microsomal preparations [39,40,81–83]) where the protocol would not have been suitable to study both membrane and microsomal proteins. This study clearly demonstrates that small intestinal pinch biopsies provide a suitable starting material. Various protein quantification methods exist including absolute quantification (AQUA) peptides or quantitative concatemers (QConCAT), this study used the QConCAT approach due to the time and cost savings enabled in this work and to provide a comparison to previous similar studies [21,32,36,37]. The QconCAT approach has been used for more than fifteen years and is well established [84,85]. Although this study did not evaluate method accuracy for QConCAT, this has been demonstrated in literature using ELISA methods [36]. Despite this, we feel that this is not an issue as using the QconCAT is a well-established approach and the focus on the paper is mainly to demonstrate the feasibility aspect of using a QconCAT and microflow to obtain preliminary ontogeny data. Thus, quantification studies on DMET protein quantification via LC-MS/MS can use intestinal pinch biopsies which are easier to collect and can widen the pool of participants in a study which enables analysis of healthy tissue taken from paediatric participants where biopsies were collected as part of a clinical investigation, rather than large tissue from paediatric participants with diagnosed comorbidities. However, the current work here is limited by the lack of repeat injections of paediatric samples (which meant method precision determination was not feasible), as this was not possible due to the minimal biopsy sizes ($17.85 \pm 6.41$ mg). All samples were measured and processed in one batch.

As such, these data should be used as preliminary values in anticipation of bigger studies and more rigorous validation strategies as used in clinical and GMP testing. These future studies should also aim to include jejunal or ileal tissue, rather than duodenal as this is rarely the major site for drug absorption due to the short transit. For this study, only duodenal samples were available, which are still of interest as predictive software incorporate duodenal characteristics in their models.

Secondly, this is the first report to use a QconCAT standard that enables quantification for both transporters and metabolising enzymes in one protein, making simultaneous quantification possible in a simplified method. Although been used previously to quantify DMET proteins in adult small intestine, there was no QconCAT developed before that contains peptide sequences for the three DMET-protein families (transporters, CYP and UGT-enzymes) [86]. Developing a single QconCAT allows for a superior method to compare and interrogate protein correlations between the different families as the standard peptides are generated in a 1:1 ratio, compared to multiple spiking event with separate peptides. The limitation of using a QconCAT is the loss of flexibility when target proteins are expressed in very different levels. As DMET-abundance in literature are reported in the range of 0.1–100 pmol/mg protein [21,32], a similar spike level was chosen in this study.

The samples were normalised to the enterocytic marker villin-1 [87], as there is a lack of ontogeny reported for this protein [20,29]. This is commonly done to correct for differences in sampling procedures and the heterogeneity of the intestinal tissue [29,47–49,88] The light-to-heavy ratio for the proteotypic peptide of villin-1 ranged from 0.13 to 1.5 (12-fold range) and most peptides could be quantified relatively to QconCAT, indicating that a suitable spike-level was chosen prior to LC-MS/MS.

This study extrapolated established protocols (cryogrinding, normal centrifugation steps, FASP digestion and quantification with a QconCAT [21,32]) from a nanoflow rate (300 nL/min) to a high-end microflow rate (0.5 mL/min). Previous proteomic studies where a microflow (0.3 mL/min) was used before, only targeted $n < 16$ peptides [20,22,39]. More commonly, a nanoflow is used in proteomic research [40]. Increasing a nanoflow to a microflow flow can improve peptide

retention [89] and separation, diminish ion suppression and allow for thinner chromatographic peaks [90]. Additionally, this method also offers opportunities to use a wider selection of apparatus for DMET protein quantification, as high-end LC instruments are more common and accessible to a larger scientific audience.

## 5. Conclusion

Overall, this study provides a simplified method for studying intestinal proteins, using pinch biopsies, a microflow chromatographic system and a unique heavy standard which can be added to the samples in a single spiking event. Intestinal CYP3A4 was the most abundant CYP-enzyme and UGT2B17 the most abundant UGT in paediatric duodenal samples. Significant trends with age were detected for CYP3A4 and CES2, in line with literature. Further work includes collecting more paediatric samples, with emphasis on recruiting neonatal and infant participants. The data from this study also suggests that it is safe to extrapolate DMET-abundancy values from adults to paediatric populations $>$ 2 years of age and strengthens the input values currently used in PBPK modelling. The clinical impact of the newfound intestinal abundancy data on the PK profile of DMET-substrates should be investigated via PBPK modelling. This paper provided novel data on the expression of DMETs in the paediatric population where data is lacking, and demonstrated the feasibility of obtaining such data using a multiplexed detection method and a QconCAT standard employing a microflow system. Future work should now focus on increasing the sample size to both confirm and validate these findings in preparation for incorporation into predictive models. They should include establishing method validation strategies (such as repeatability, accuracy and precision), using sample replicates of bigger biopsies or a pooled sample approach.

## CRediT authorship contribution statement

**Jan Goelen:** Conceptualization, Methodology, Investigation. **Gillian Farrell:** Methodology, Investigation. **Jonathan McGeehan:** Methodology. **Christopher M. Titman:** Methodology. **Nicholas J. W. Rattray:** Methodology, Supervision. **Trevor N. Johnson:** Conceptualization, Supervision. **Richard D. Horniblow:** Conceptualization, Supervision. **Hannah K. Batchelor:** Conceptualization, Supervision.

## Declaration of Competing Interest

The authors declare that they have no known competing financial interests or personal relationships that could have appeared to influence the work reported in this paper.

## Data availability

Data will be made available on request.

## Acknowledgments

Certara funded this work as a PhD project for J. G.. The authors thank Gopal Pawar for his advice regarding isolation methods. The authors also thank PolyQuant and Florian Christoph Sigloch for their contribution in synthesising the PaedCAT. The authors would like to thank the Strathclyde Centre of Molecular Bioscience for access to instrumentation and Shimazu-UK for advice on method development.

## Appendix A. Supplementary material

Supplementary data to this article can be found online at https://doi.org/10.1016/j.ejpb.2023.08.011.

## References

[1] J. Van Den Abeele, et al., Gastric fluid composition in a paediatric population: Age-dependent changes relevant for gastrointestinal drug disposition, Eur. J. Pharm. Sci. 123 (2018) 301–311.
[2] H.K. Batchelor, N. Fotaki, S. Klein, Paediatric oral biopharmaceutics: key considerations and current challenges, Adv. Drug Deliv. Rev. 73 (2014) 102–126.
[3] H.K. Batchelor, J.F. Marriott, Formulations for children: problems and solutions, Br. J. Clin. Pharmacol. 79 (3) (2015) 405–418.
[4] M. Van Den Driessche, et al., Lactose-[13C]ureide breath test: a new, noninvasive technique to determine orocecal transit time in children, J. Pediatr. Gastroenterol. Nutr. 31 (4) (2000) 433–438.
[5] T.N. Johnson, B.G. Small, K. Rowland Yeo, Increasing application of pediatric physiologically based pharmacokinetic models across academic and industry organizations, CPT Pharmacometrics Syst. Pharmacol. 11 (3) (2022) 373–383.
[6] J.D. Momper, Y. Mulugeta, G.J. Burckart, Failed Pediatric Drug Development Trials, Clin. Pharmacol. Ther. 98 (3) (2015) 245–251.
[7] V. Yellepeddi, et al., State-of-the-Art Review on Physiologically Based Pharmacokinetic Modeling in Pediatric Drug Development, Clin. Pharmacokinet. 58 (1) (2019) 1–13.
[8] M. Van der Veken, et al., Practical and operational considerations related to paediatric oral drug formulation: An industry survey, Int. J. Pharm. 618 (2022), 121670.
[9] A.R. Maharaj, A.N. Edginton, Physiologically based pharmacokinetic modeling and simulation in pediatric drug development, CPT Pharmacometrics Syst. Pharmacol. 3 (11) (2014) e150.
[10] M. Jamei, et al., The Simcyp population-based ADME simulator, Expert Opin. Drug Metab. Toxicol. 5 (2) (2009) 211–223.
[11] L.F.M. Verscheijden, et al., Physiologically-based pharmacokinetic models for children: Starting to reach maturation? Pharmacol. Ther. (2020), 107541.
[12] T.N. Johnson, et al., Development and applications of a physiologically-based model of paediatric oral drug absorption, Eur. J. Pharm. Sci. 115 (2018) 57–67.
[13] M. Cella, et al., Paediatric drug development: are population models predictive of pharmacokinetics across paediatric populations? Br. J. Clin. Pharmacol. 72 (3) (2011) 454–464.
[14] K.M. Giacomini, et al., Membrane transporters in drug development, Nat. Rev. Drug Discov. 9 (3) (2010) 215–236.
[15] C. Stillhart, et al., Impact of gastrointestinal physiology on drug absorption in special populations—An UNGAP review, Eur. J. Pharm. Sci. 147 (2020), 105280.
[16] H.K. Batchelor, J.F. Marriott, Paediatric pharmacokinetics: key considerations, Br. J. Clin. Pharmacol. 79 (3) (2013) 395–404.
[17] K.L. Brouwer, et al., Human Ontogeny of Drug Transporters: Review and Recommendations of the Pediatric Transporter Working Group, Clin. Pharmacol. Ther. 98 (3) (2015) 266–287.
[18] M.J. Zamek-Gliszczynski, et al., Transporters in Drug Development: 2018 ITC Recommendations for Transporters of Emerging Clinical Importance, Clin. Pharmacol. Ther. 104 (5) (2018) 890–899.
[19] K.M. Hillgren, et al., Emerging transporters of clinical importance: an update from the International Transporter Consortium, Clin. Pharmacol. Ther. 94 (1) (2013) 52–63.
[20] M. Kiss, et al., Ontogeny of Small Intestinal Drug Transporters and Metabolizing Enzymes Based on Targeted Quantitative Proteomics, Drug Metab. Dispos. (2021) p. DMD-AR-2021-000559.
[21] N. Couto, et al., Quantitative Proteomics of Clinically Relevant Drug-Metabolizing Enzymes and Drug Transporters and Their Intercorrelations in the Human Small Intestine, Drug Metab. Dispos. 48 (4) (2020) 245–254.
[22] M. Drozdzik, et al., Protein abundance of clinically relevant multidrug transporters along the entire length of the human intestine, Mol. Pharm. 11 (10) (2014) 3547–3555.
[23] T. de Waal, et al., The impact of inflammation on the expression of drug transporters and metabolic enzymes in colonic tissue from ulcerative colitis patients, Int. J. Pharm. 628 (2022), 122282.
[24] M. Estudante, et al., Intestinal drug transporters: an overview, Adv. Drug Deliv. Rev. 65 (10) (2013) 1340–1356.
[25] B.B. Madison, et al., cis Elements of the Villin Gene Control Expression in Restricted Domains of the Vertical (Crypt) and Horizontal (Duodenum, Cecum) Axes of the Intestine*, J. Biol. Chem. 277 (36) (2002) 33275–33283.
[26] I.M. Glynn, Annual review prize lecture. 'All hands to the sodium pump', J. Physiol. 462 (1993) 1–30.
[27] M. Taketani, et al., Carboxylesterase in the liver and small intestine of experimental animals and human, Life Sci. 81 (11) (2007) 924–932.
[28] E.J. Streekstra, et al., Application of proteomics to understand maturation of drug metabolizing enzymes and transporters for the optimization of pediatric drug therapy, Drug Discov. Today Technol. 39 (2021) 31–48.
[29] T.N. Johnson, et al., Enterocytic CYP3A4 in a paediatric population: developmental changes and the effect of coeliac disease and cystic fibrosis, Br. J. Clin. Pharmacol. 51 (5) (2001) 451–460.
[30] N. Couto, et al., Quantification of Proteins Involved in Drug Metabolism and Disposition in the Human Liver Using Label-Free Global Proteomics, Mol. Pharm. 16 (2) (2019) 632–647.
[31] M. Drozdzik, et al., Protein Abundance of Clinically Relevant Drug Transporters in the Human Liver and Intestine: A Comparative Analysis in Paired Tissue Specimens, Clin. Pharmacol. Ther. 105 (5) (2019) 1204–1212.
[32] M.D. Harwood, et al., Application of an LC-MS/MS method for the simultaneous quantification of human intestinal transporter proteins absolute abundance using a QconCAT technique, J. Pharm. Biomed. Anal. 110 (2015) 27–33.

[33] C. Groer, et al., LC-MS/MS-based quantification of clinically relevant intestinal uptake and efflux transporter proteins, J. Pharm. Biomed. Anal. 85 (2013) 253–261.
[34] S. Oswald, et al., Mass spectrometry-based targeted proteomics as a tool to elucidate the expression and function of intestinal drug transporters, AAPS J. 15 (4) (2013) 1128–1140.
[35] R. Aebersold, M. Mann, Mass spectrometry-based proteomics, Nature 422 (6928) (2003) 198–207.
[36] B. Achour, et al., Simultaneous Quantification of the Abundance of Several Cytochrome P450 and Uridine 5'-Diphospho-Glucuronosyltransferase Enzymes in Human Liver Microsomes Using Multiplexed Targeted Proteomics, Drug Metab. Dispos. (2014) p. dmd.113.055632.
[37] M.R. Russell, et al., Alternative fusion protein strategies to express recalcitrant QconCAT proteins for quantitative proteomics of human drug metabolizing enzymes and transporters, J. Proteome Res. 12 (12) (2013) 5934–5942.
[38] E. El-Khateeb, et al., Quantitative mass spectrometry-based proteomics in the era of model-informed drug development: Applications in translational pharmacology and recommendations for best practice, Pharmacol. Ther. 203 (2019), 107397.
[39] C. Gröer, et al., Absolute protein quantification of clinically relevant cytochrome P450 enzymes and UDP-glucuronosyltransferases by mass spectrometry-based targeted proteomics, J. Pharm. Biomed. Anal. 100 (2014) 393–401.
[40] G.N. Asher, J.K. Fallon, P.C. Smith, UGT concentrations in human rectal tissue after multidose, oral curcumin, Pharmacol. Res. Perspect. 4 (2) (2016) e00222.
[41] H. Al Feteisi, et al., Choice of LC-MS Methods for the Absolute Quantification of Drug-Metabolizing Enzymes and Transporters in Human Tissue: a Comparative Cost Analysis, AAPS J. 17 (2) (2015) 438–446.
[42] R.J. Beynon, et al., Multiplexed absolute quantification in proteomics using artificial QCAT proteins of concatenated signature peptides, Nat. Methods 2 (8) (2005) 587–589.
[43] Z.M. Al-Majdoub, et al., Quantification of Proteins Involved in Intestinal Epithelial Handling of Xenobiotics, Clin. Pharmacol. Ther. (2020).
[44] M. Guimarães, et al., Biopharmaceutical considerations in paediatrics with a view to the evaluation of orally administered drug products – a PEARRL review, J. Pharm. Pharmacol. 71 (4) (2019) 603–642.
[45] Use, C.f.M.P.f.H., Reflection paper: formulations of choice for the paediatric population. EMEA, London, 2006.
[46] J. Kamiie, et al., Quantitative atlas of membrane transporter proteins: development and application of a highly sensitive simultaneous LC/MS/MS method combined with novel in-silico peptide selection criteria, Pharm. Res. 25 (6) (2008) 1469–1483.
[47] A.G. Pinto, et al., Diltiazem inhibits human intestinal cytochrome P450 3A (CYP3A) activity in vivo without altering the expression of intestinal mRNA or protein, Br. J. Clin. Pharmacol. 59 (4) (2005) 440–446.
[48] E. Miyauchi, et al., Quantitative Atlas of Cytochrome P450, UDP-Glucuronosyltransferase, and Transporter Proteins in Jejunum of Morbidly Obese Subjects, Mol. Pharm. 13 (8) (2016) 2631–2640.
[49] P.B. Watkins, The barrier function of CYP3A4 and P-glycoprotein in the small bowel, Adv. Drug Deliv. Rev. 27 (2) (1997) 161–170.
[50] B.J. Danesh, et al., Comparison of weight, depth, and diagnostic adequacy of specimens obtained with 16 different biopsy forceps designed for upper gastrointestinal endoscopy, Gut 26 (3) (1985) 227–231.
[51] A. Grangeon, et al., Determination of CYP450 Expression Levels in the Human Small Intestine by Mass Spectrometry-Based Targeted Proteomics, Int. J. Mol. Sci. 22 (23) (2021) 12791.
[52] M. Drozdzik, et al., Protein Abundance of Clinically Relevant Drug-Metabolizing Enzymes in the Human Liver and Intestine: A Comparative Analysis in Paired Tissue Specimens, Clin. Pharmacol. Ther. 104 (3) (2018) 515–524.
[53] T. Akazawa, et al., High Expression of UGT1A1/1A6 in Monkey Small Intestine: Comparison of Protein Expression Levels of Cytochromes P450, UDP-Glucuronosyltransferases, and Transporters in Small Intestine of Cynomolgus Monkey and Human, Mol. Pharm. 15 (1) (2018) 127–140.
[54] M.F. Paine, et al., The human intestinal cytochrome P450 "pie", Drug Metab. Dispos. 34 (5) (2006) 880–886.
[55] Y.T. Chen, et al., Ontogenic expression of human carboxylesterase-2 and cytochrome P450 3A4 in liver and duodenum: postnatal surge and organ-dependent regulation, Toxicology 330 (2015) 55–61.
[56] R.N. Hines, P.M. Simpson, D.G. McCarver, Age-Dependent Human Hepatic Carboxylesterase 1 (CES1) and Carboxylesterase 2 (CES2) Postnatal Ontogeny, Drug Metab. Dispos. 44 (7) (2016) 959–966.
[57] S.C. Laizure, et al., The role of human carboxylesterases in drug metabolism: have we overlooked their importance? Pharmacotherapy 33 (2) (2013) 210–222.
[58] E. Jacqz-Aigrain, P. Burtin, Clinical pharmacokinetics of sedatives in neonates, Clin. Pharmacokinet. 31 (6) (1996) 423–443.
[59] J.L. Blumer, Clinical pharmacology of midazolam in infants and children, Clin. Pharmacokinet. 35 (1) (1998) 37–47.
[60] I. Ince, et al., A novel maturation function for clearance of the cytochrome P450 3A substrate midazolam from preterm neonates to adults, Clin. Pharmacokinet. 52 (7) (2013) 555–565.
[61] S.N. de Wildt, et al., Ontogeny of midazolam glucuronidation in preterm infants, Eur. J. Clin. Pharmacol. 66 (2) (2010) 165–170.
[62] S.N. de Wildt, et al., Pharmacodynamics of midazolam in pediatric intensive care patients, Ther. Drug Monit. 27 (1) (2005) 98–102.
[63] S.N. de Wildt, et al., Population pharmacokinetics and metabolism of midazolam in pediatric intensive care patients, Crit. Care Med. 31 (7) (2003) 1952–1958.
[64] S.N. de Wildt, et al., Pharmacokinetics and metabolism of oral midazolam in preterm infants, Br. J. Clin. Pharmacol. 53 (4) (2002) 390–392.
[65] S.N. de Wildt, et al., Pharmacokinetics and metabolism of intravenous midazolam in preterm infants, Clin. Pharmacol. Ther. 70 (6) (2001) 525–531.
[66] K. Payne, et al., The pharmacokinetics of midazolam in paediatric patients, Eur. J. Clin. Pharmacol. 37 (3) (1989) 267–272.
[67] M.J. Brill, et al., Midazolam pharmacokinetics in morbidly obese patients following semi-simultaneous oral and intravenous administration: a comparison with healthy volunteers, Clin. Pharmacokinet. 53 (10) (2014) 931–941.
[68] J.M. Brussee, et al., First-Pass CYP3A-Mediated Metabolism of Midazolam in the Gut Wall and Liver in Preterm Neonates, CPT Pharmacometrics Syst. Pharmacol. 7 (6) (2018) 374–383.
[69] B. Prasad, et al., Toward a Consensus on Applying Quantitative Liquid Chromatography-Tandem Mass Spectrometry Proteomics in Translational Pharmacology Research: A White Paper, Clin. Pharmacol. Ther. 106 (3) (2019) 525–543.
[70] D.K. Bhatt, B. Prasad, Critical Issues and Optimized Practices in Quantification of Protein Abundance Level to Determine Interindividual Variability in DMET Proteins by LC-MS/MS Proteomics, Clin. Pharmacol. Ther. 103 (4) (2018) 619–630.
[71] C. Wegler, et al., Variability in Mass Spectrometry-based Quantification of Clinically Relevant Drug Transporters and Drug Metabolizing Enzymes, Mol. Pharm. 14 (9) (2017) 3142–3151.
[72] J.C. Silva, et al., Quantitative proteomic analysis by accurate mass retention time pairs, Anal. Chem. 77 (7) (2005) 2187–2200.
[73] N. Couto, et al., Correction to "Quantitative Proteomics of Clinically Relevant Drug-Metabolizing Enzymes and Drug Transporters and Their Intercorrelations in the Human Small Intestine", Drug Metab. Dispos. 48 (5) (2020) 407.
[74] T.G. Tucker, et al., Absolute immunoquantification of the expression of ABC transporters P-glycoprotein, breast cancer resistance protein and multidrug resistance-associated protein 2 in human liver and duodenum, Biochem. Pharmacol. 83 (2) (2012) 279–285.
[75] M.G. Mooij, et al., Ontogeny of human hepatic and intestinal transporter gene expression during childhood: age matters, Drug Metab. Dispos. 42 (8) (2014) 1268–1274.
[76] A. Konieczna, et al., Differential expression of ABC transporters (MDR1, MRP1, BCRP) in developing human embryos, J. Mol. Histol. 42 (6) (2011) 567–574.
[77] M. Fakhoury, et al., mRNA expression of MDR1 and major metabolising enzymes in human fetal tissues, Drug Metab. Pharmacokinet. 24 (6) (2009) 529–536.
[78] M. Fakhoury, et al., LOCALIZATION AND mRNA EXPRESSION OF CYP3A AND P-GLYCOPROTEIN IN HUMAN DUODENUM AS A FUNCTION OF AGE, Drug Metab. Dispos. 33 (11) (2005) 1603–1607.
[79] Y. Miki, et al., Steroid and xenobiotic receptor (SXR), cytochrome P450 3A4 and multidrug resistance gene 1 in human adult and fetal tissues, Mol. Cell. Endocrinol. 231 (1–2) (2005) 75–85.
[80] D.R. de Waart, et al., Oral availability of cefadroxil depends on ABCC3 and ABCC4, Drug Metab. Dispos. 40 (3) (2012) 515–521.
[81] O.J. Hatley, et al., Quantifying gut wall metabolism: methodology matters, Biopharm. Drug Dispos. 38 (2) (2017) 155–160.
[82] Y. Sato, et al., Optimized methods for targeted peptide-based quantification of human uridine 5'-diphosphate-glucuronosyltransferases in biological specimens using liquid chromatography-tandem mass spectrometry, Drug Metab. Dispos. 42 (5) (2014) 885–889.
[83] D.E. Harbourt, et al., Quantification of human uridine-diphosphate glucuronosyl transferase 1A isoforms in liver, intestine, and kidney using nanobore liquid chromatography-tandem mass spectrometry, Anal. Chem. 84 (1) (2012) 98–105.
[84] M. Gavage, et al., Comparative study of concatemer efficiency as an isotope-labelled internal standard for allergen quantification, Food Chem. 332 (2020), 127413.
[85] T.A. Zimmerman, et al., Quantification of Transferrin in Human Serum Using Both QconCAT and Synthetic Internal Standards, Anal. Chem. 85 (21) (2013) 10362–10368.
[86] A.M. Vasilogianni, et al., A family of QconCATs (Quantification conCATemers) for the quantification of human pharmacological target proteins, J. Proteomics 261 (2022), 104572.
[87] A.B. West, et al., Localization of villin, a cytoskeletal protein specific to microvilli, in human ileum and colon and in colonic neoplasms, Gastroenterology 94 (2) (1988) 343–352.
[88] H. Zhang, et al., Regional Proteomic Quantification of Clinically Relevant Non-Cytochrome P450 Enzymes along the Human Small Intestine, Drug Metab. Dispos. 48 (7) (2020) 528–536.
[89] O.V. Krokhin, V. Spicer, Generation of accurate peptide retention data for targeted and data independent quantitative LC-MS analysis: Chromatographic lessons in proteomics, Proteomics 16 (23) (2016) 2931–2936.
[90] J. Lenco, et al., Conventional-Flow Liquid Chromatography-Mass Spectrometry for Exploratory Bottom-Up Proteomic Analyses, Anal. Chem. 90 (8) (2018) 5381–5389.